Interface dynamics and kinetic roughening in fractals

J. Asikainen,[1] S. Majaniemi,[1] M. Dubé,[2] and T. Ala-Nissila[1,3]
[1]*Helsinki Institute of Physics and Laboratory of Physics, Helsinki University of Technology, P.O. Box 1100, FIN-02015 HUT, Espoo, Finland*
[2]*Department of Physics, McGill University, 3600 University Street, Montréal, Quebéc, Canada H3A 2T8*
[3]*Department of Physics, Brown University, Providence, Rhode Island 02912-1843*
(Received 7 December 2001; published 20 May 2002)

We consider the dynamics and kinetic roughening of single-valued interfaces in two-dimensional fractal media. Assuming that the local height difference distribution function of the fronts obeys Levý statistics with a well-defined power-law decay exponent, we derive analytic expressions for the local scaling exponents. We also show that the kinetic roughening of the interfaces displays anomalous scaling and multiscaling in the relevant correlation functions. For invasion percolation models, the exponents can be obtained from the fractal geometry of percolation clusters. Our predictions are in excellent agreement with numerical simulations.

DOI: 10.1103/PhysRevE.65.052104 PACS number(s): 68.35.Ct, 47.53.+n, 61.43.Hv, 68.35.Ja

Kinetic roughening of driven interfaces is an ubiquitous phenomenom in nature, with applications varying from the crystal growth [1] to fluid invasion in porous media [2]. In many cases of interest, there is a description of such processes in terms of a stochastic equation of motion for the (single-valued) height function $h(\vec{x},t)$. Such equations of motion can be local, such as the well-known Kardar-Parisi-Zhang (KPZ) equation [3] and its variants, or nonlocal due to, e.g., an underlying conservation law in the system [4]. Both classes of equations typically lead to power-law scaling of the relevant height correlation functions, with associated scaling exponents whose values are known exactly in some special cases.

There exist interesting connections between kinetic roughening and more general theories of scale-invariant structures [1,5]. An important special case is the connection to percolation theory [6] for fronts that become pinned due to quenched disorder [2]. There are two important universality classes arising from the quenched KPZ description near pinning, namely, the isotropic percolation (IP) and directed percolation depinning (DPD) cases [7]. These two differ by their scaling exponents, as well as by the behavior of the nonlinear term in the underlying KPZ equation. Another case related to percolation is that of the propagation of a single-valued interface in a background, which itself undergoes a percolation transition and is thus a fractal [8,9]. This situation arises in models of slow combustion fronts [8], or ''forest fire'' lattice models [9]. In this isotropic percolation depinning (IPD) case [9], some of the scaling exponents can be directly related to the geometric properties of the underlying percolation cluster similar to the DPD case [7]. However, in the IPD limit there exists no KPZ type of description for the interface dynamics. Nontrivial fractal structures emerge from various growth models as well, including diffusion limited aggregation [10] and various oblique-incidence ballistic growth models [1]. The current understanding of the roughening properties of fronts in such fractals is still rather incomplete.

In this work, our aim is to examine the problem of kinetic roughening of *single-valued* fronts in fractal media. To this end, we study front propagation and kinetic roughening in IP models [11]. They constitute an important and widely studied class of percolation theory. The IP is a dynamic percolation process that describes the displacement of one fluid by another in a porous medium in the limit where capillary forces dominate the viscous forces [6]. IP can be divided in two cases: one with trapping (TIP) and the other without it (NTIP). TIP describes a situation in which the defender fluid is incompressible, and thus invasion process terminates in regions fully surrounded by the invading fluid. The NTIP model, on the other hand, is consistent with the case where the defending fluid is compressible. An important property of the NTIP model is that it is believed to to be equivalent to ordinary percolation [12]. The temporal development of IP clusters has been studied in Refs. [13,14], and self-organization and kinetic roughening with local slope constraints in Ref. [15].

We first present results of numerical simulations of the lattice model of NTIP, where we calculate the various correlation functions of the single-valued heights associated with the invading front, and estimate the corresponding scaling exponents. We find that there is anomalous scaling and multiscaling in the temporal and spatial correlation functions. We argue that this can be generally explained by the underlying Lévy statistics of the jumps of neighboring interface heights. The properties of the Lévy distribution can be expressed solely in terms of the geometry of the fractal. From this we derive exact expressions for the *local* scaling exponents, which turn out to depend on both the form of the Lévy distribution and the *global* roughening exponents. Our numerical simulations are in excellent agreement with the theoretical predictions.

The numerical simulations of the NITP lattice model were done on a two-dimensional (2D) square lattice of size $L_x \times L_y$, with $L_x = 32-4096$ and $L_y = L_x - 4L_x$. Our simulation method is basically the same as in Refs. [16–18]. The main algorithmic aspect is that the list of active growth sites is implemented via a balanced binary search tree. By this method, the insertion and deletion operations on the list can be performed in time $\propto \ln(n)$, where n is the list size.

In the model, we define a set of single-valued local interface heights $\{h(x_i,t)\}_{i=1}^{L_x}$ at x_i by the highest invaded lattice site [9] (see Fig. 1). The *global* interface width $w_q(t,L_x)$ can be defined by

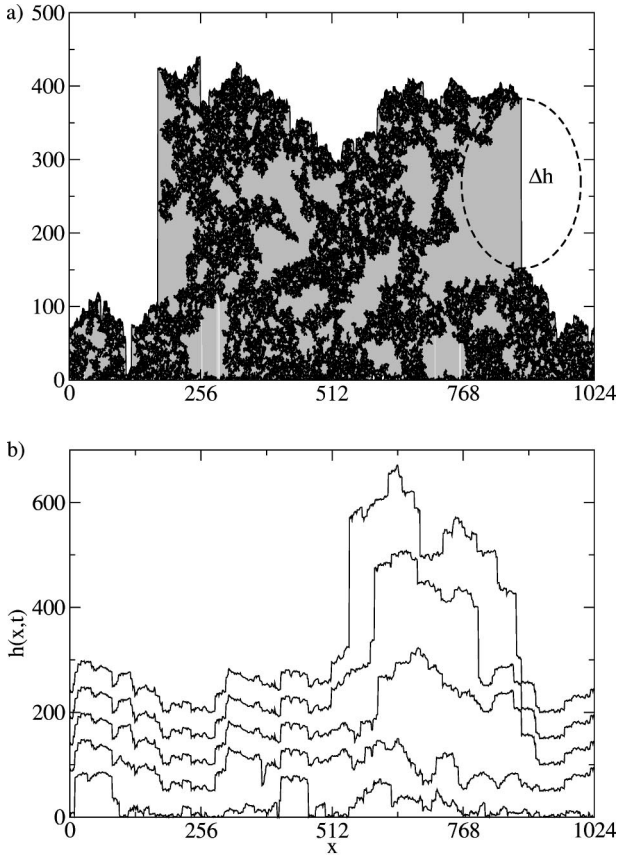

FIG. 1. (a) A typical configuration of an NTIP cluster. A large overhang of size Δh is outlined with an ellipse. The gray area under the solid line shows how overhangs are cut off. Both axes are in units of latice constant a, as in (b). (b) A set of five consecutive height profiles separated by time t corresponding to 10 monolayers is shown. Each curve has been shifted by 50 lattice units for clarity.

$$w_q(t,L_x) \equiv \langle \overline{[h(x,t)-\overline{h}(t)]^q} \rangle^{1/q}, \tag{1}$$

where the overbar denotes spatial averaging over the system of size L_x and angular brackets denote configuration averaging. The global width satisfies the Family-Viscek scaling ansatz [19] $w(t,L) \sim t^{\beta} f(t/L^z)$ for all q, where the scaling function $f(u \to 0) = \text{const}$ and $f(u \to \infty) \propto u^{-\beta}$. Here, β defines the (global) growth exponent. The dynamic exponent z describes the scaling of saturation time t_s with system size, $t_s \sim L^z$, and β and z are connected through the global roughness exponent χ as $\beta = \chi/z$ [2].

For the IPD case, it has been shown that $\chi = 1$ due to the isotropy of the underlying percolation cluster [9]. This argument should hold here, too, and we indeed find numerically that $\chi = 0.99 \pm 0.02$. We also measured β and find that $w_2(t)$ grows linearly in time, i.e., $\beta = 1.00 \pm 0.03$. This indicates that the dynamic exponent $z = 0.99 \pm 0.05$. This differs from the DPD and IPD cases, where $z = d_{\min}$, and $d_{\min} \approx 1.13$ is the minimum distance exponent of the underlying 2D percolation cluster [9,20].

To study the *local* properties of the growing interfaces, the qth order height difference correlation function is defined as

$$G_q(x,t) = \langle \overline{|h(x_0,t) - h(x_0+x,t)|^q} \rangle^{1/q}, \tag{2}$$

with G_q satisfying the anomalous scaling relation [9,21]

$$G_q(x,t) = \xi^{\alpha_q} x^{\chi_q} f_q(x/\xi). \tag{3}$$

Here, the scaling function $f_q(u \to 0) = \text{const}$ and $f_q(u \to \infty) \propto u^{-\chi_q}$ [9]. The exponents α_q define the so-called anomaly exponents, and χ_q's define local roughness exponents. We have also calculated the average nearest neighbor height difference function $\sigma_q(t)$, defined by [22]

$$\sigma_q(t) = \langle \overline{|h(x_{i+1},t) - h(x_i,t)|^q} \rangle^{1/q}, \tag{4}$$

which at early times follows the scaling relation

$$\sigma_q \sim \xi^{\alpha_q} \sim t^{\alpha_q/z} \sim t^{\beta_q}, \tag{5}$$

where β_q are the local growth exponents. One can also define the time-dependent qth order height-height fluctuation correlation function

$$C_q(t) = \langle \overline{[\delta h(x,t_0) - \delta h(x,t_0+t)]^q} \rangle^{1/q}, \tag{6}$$

where $\delta h \equiv h - \overline{h}$ is the deviation from the average height. In the saturated regime, one expects C_q to scale as $C_q \sim t^{\tilde{\beta} q}$ at early times, and to saturate to a system size dependent value at large times.

In Figs. 2(a) and 2(b) we show our numerical results for some relevant correlation functions. The measured values for the corresponding scaling exponents are also listed in Table I. Anomalous scaling and multiscaling of the correlation functions are evident in the data. We have numerically calculated the distribution function $P(\Delta h)$ for local slopes, where $\Delta h \equiv |h(x_{i+1}) - h(x_i)|$. It shows a clear power-law dependence on the jump size, $P(\Delta h = \ell) \sim \ell^{-\alpha}$, and we find that $\alpha = 2.00 \pm 0.05$.

To theoretically explain these results, we consider the geometry of the underlying percolation cluster. The single-valued interface consists of pieces of the hull of the percolation cluster, separated by vertical jumps as shown in Fig. 1(a). At a point $\vec{x}$ on the invasion front, a jump of size $\Delta h \gg 1$ means that there is an overhang below $\vec{x}$. The probability of finding such an overhang can be directly found using results from percolation theory. At the threshold, the probability per site of finding a cluster of size s scales as $n_s \sim s^{-\tau}$, and the linear size ℓ of the cluster of size s scales as $\ell \sim s^{1/D}$, where D is the fractal dimension of the cluster [6]. Thus for a jump of the size $\Delta h = \ell$, $P(\ell)$ is proportional to the probability of finding a cluster of size ℓ (see Fig. 1). The cluster of this size has $s \sim \ell^D$ sites. The probability of finding a cluster of s sites scales as $n_s s \sim s^{-\tau+1}$. Finally, taking into account the scaling of the mass of the cluster with its size, we have that

$$P(\ell) \sim \ell^{(-\tau+1)D} = \ell^{-2} \tag{7}$$

by using the exact values of $D = 91/48$ and $\tau = 187/91$ from percolation theory [6]. This is in excellent agreement with our simulations. This means that the local interface slopes

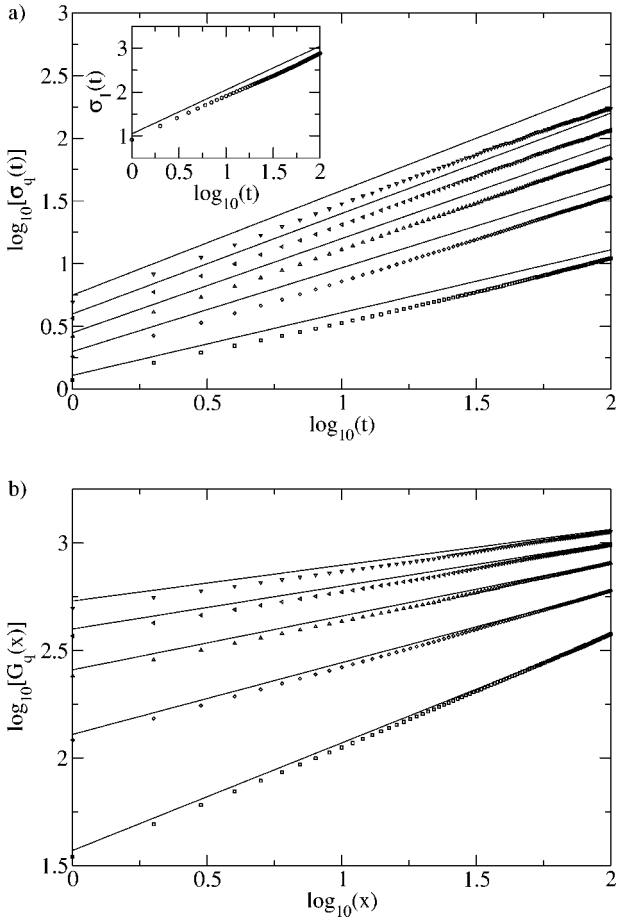

FIG. 2. (a) The local height difference correlation functions $\sigma_q(t)$. The inset shows the logarithmic behavior for $q=1$; time is in units of the number of monolayers (ML); system size is 1024×2048. (b) The correlation functions $G_q(x)$ in units of lattice spacing a (in the saturated regime); system size is 4096×16384. In both cases, from bottom to top $q=2,3,4,5$, and 6. The solid lines denote the theoretical predictions of Table I.

follow an anomalous Lévy distribution in contrast to, e.g., the KPZ case, where the distribution is of Gaussian (random-walk) type [23].

Equation (7) can now be used to derive the scaling exponents in the following way. Let $|\Delta h|_{max}$ denote the largest of the local slopes. We can now assume that

TABLE I. The local scaling exponents from numerical simulations of the NTIP model. Analytic prediction is shown in the lower part of the table.

q	β_q	$\tilde{\beta}_q$	χ_q
1	$O(\log)$	0.95 ± 0.04	0.86 ± 0.01
2	0.51 ± 0.05	0.51 ± 0.01	0.51 ± 0.02
3	0.67 ± 0.04	0.33 ± 0.02	0.34 ± 0.02
4	0.73 ± 0.02	0.24 ± 0.01	0.26 ± 0.01
5	0.75 ± 0.03	0.19 ± 0.02	0.20 ± 0.02
6	0.77 ± 0.02	0.16 ± 0.02	0.17 ± 0.02
	$1-1/q$	$1/q$	$1/q$

$$[\sigma_q(t)]^q \approx \int_0^{|\Delta h|_{max}} d\Delta h P(\Delta h)(\Delta h)^q. \tag{8}$$

For the maximum height differences, $|\Delta h|_{max}\sim w_\infty(t)\sim t^{\beta_\infty}$, where $\beta_\infty=\beta=1$ for the present model. Thus, for different q's we have

$$\sigma_q(t)\sim\begin{cases}\ln t & \text{for } q=1,\\ t^{1-1/q} & \text{for } q>1,\end{cases} \tag{9}$$

which means that the local growth exponents are given by $\beta_1=0$ $[O(\log)]$ and $\beta_q=1-1/q$ for $q>1$. These predictions are in excellent agreement with our numerical data in Table I. The local roughness exponent can be obtained by combining the scaling of $\sigma_q(t)$ and $G_q(x,t)$ [Eqs. (3) and (5) with $x\approx\xi\approx L$]. Using $\chi_q+\alpha_q=\chi=1$ and $z=1$ yields

$$\chi_q=1/q, \tag{10}$$

which is again in excellent agreement with our data.

To explain the scaling behavior of C_q we define a generalized correlation function $\tilde{C}_q(x,t_0,t)\equiv\langle|\delta h(x_0,t_0)-\delta h(x_0+x,t_0+t)|^q\rangle^{1/q}$. It has the following limits: $\tilde{C}_q(x,t_0,0)=G_q(x,t_0)$, $\tilde{C}_q(1,t_0,0)=\sigma_q(t_0)$, and $\tilde{C}_q(0,t_0,t)=C_q(t_0,t)$. We propose that $\tilde{C}_q(x,t_0,t)=\xi(t_0)^{\alpha_q}x^{\chi_q}\tilde{f}_q(u_1,u_2)$, where we have defined $u_1\equiv x/\xi(t_0)$ and $u_2\equiv t/t_0$. First, for $u_2=0$, we must obtain the scaling form of $G_q(x,t_0)$. Therefore, $\tilde{f}_q(u_1,u_2=0)=f_q(u_1)\propto u_1^{-\chi_q}$ for $u_1\gg1$. For small times t_0 this gives $G_q(x,t_0)\propto t_0^{(\alpha_q+\chi_q)/z}\propto t_0$, which we have confirmed numerically for the first few values of q. Next, we consider nonzero u_2. Taking the limit $x\to0$ of $\tilde{C}_q$ we should recover C_q. Since the x dependence must vanish we require that $\tilde{f}_q(u_1,u_2)\propto u_1^{-\chi_q}g_q(u_2)$ for $u_1\to0$. Hence, $\tilde{C}_q(x\to0,t_0,t)\propto\xi(t_0)^{\alpha_q}x^{\chi_q}u_1^{-\chi_q}g_q(u_2)\propto t_0 g_q(t/t_0)\propto C_q(t_0,t)$. This is an explict scaling *prediction* for $z=1$. We have numerically confirmed that $g_q(u_2)\propto u_2^{\tilde{\beta}_q}$ for $u_2\ll1$. This gives $\tilde{\beta}_q=\chi_q=1/q$.

We have also studied the TIP model numerically. We find that $(-\tau+1)D=-1.9\pm0.1$ and thus both the probability distribution $P(\Delta h)$ and the scaling exponents are the same for NTIP and TIP. This is not obvious since neither the fractal dimension nor the exponent τ is known exactly for TIP. Numerical estimates give $D\approx1.82$ [11], a value that is slightly lower than for the NTIP case. We are not aware of any previous numerical estimates of τ, but from our results we can estimate that $\tau=2.0\pm0.1$.

It is interesting to compare the present results with the IPD case as obtained for a "forest fire" lattice model close to percolation [9]. In both cases, $\chi=1$ due to isotropy. However, in the IPD case it was shown that $z=d_{\min}\approx1.13$ corresponding to a 2D minimum path exponent, while here $z=1$. Thus, the global *dynamical* exponents β and z of the IP case are *different* from the IPD case. However, the important point is that the *local* scaling exponents must be still given by our analytic arguments, with $\beta=1/d_{\min}$. For the IPD case,

this gives the same local roughness exponents $\chi_q = 1/q$ as in the IP case, but now the local growth exponents are given by $\beta_q = \beta(1-1/q)$, which is indeed consistent with the numerical data in Ref. [9].

To summarize, we have studied the problem of kinetic roughening of single-valued height fronts in fractals. By considering the invasion percolation model as an example, we have been able to show how the Lévy statistics of the local interface slopes generates multiscaling and anomalous scaling. We have also shown how the local scaling exponents can be analytically derived. These predictions have been verified by numerical simulations, and should be easy to measure for various physical processes, where fractal growth structures are generated. Such measurements give direct information about the fractal properties of the structures as we have shown here.

The authors want to acknowledge Ismo Koponen for helpful discussions. This work has been supported in part by the Academy of Finland through its Center of Excellence program. J.A. acknowledges the Vaisala Foundation for financial support.

[1] J. Krug, Adv. Phys. **46**, 139 (1997).
[2] A.-L. Barabási and H.E. Stanley, *Fractal Concepts in Surface Growth* (Cambridge University Press, Cambridge, 1995).
[3] M. Kardar, G. Parisi, and Y.-C. Zhang, Phys. Rev. Lett. **79**, 889 (1986).
[4] T. Salditt and H. Spohn, Phys. Rev. E **47**, 3524 (1993); J. Heinonen, I. Bukharev, T. Ala-Nissila, and J.M. Kosterlitz, *ibid.* **57**, 6851 (1998); M. Dubé, M. Rost, K.R. Elder, M. Alava, S. Majaniemi, and T. Ala-Nissila, Phys. Rev. Lett. **83**, 1628 (1999); Eur. Phys. J. B **15**, 701 (2000).
[5] M. Paczuski, S. Maslov, and P. Bak, Phys. Rev. E **53**, 414 (1996); G. Huber, M.H. Jensen, and K. Sneppen, *ibid.* **52**, R2133 (1995).
[6] D. Stauffer and A. Aharony, *Introduction to Percolation Theory*, 2nd ed. (Taylor and Francis, London, 1994).
[7] L.-H. Tang, M. Kardar, and D. Dhar, Phys. Rev. Lett. **74**, 920 (1995).
[8] N. Provatas, T. Ala-Nissila, M. Grant, K.R. Elder, and L. Piché, Phys. Rev. E **51**, 4232 (1995); J. Stat. Phys. **81**, 737 (1995).
[9] M.P. Kuittu, M. Haataja, N. Provatas, and T. Ala-Nissila, Phys. Rev. E **58**, 1514 (1998); **59**, 3774 (1999).
[10] T.A. Witten and L.M. Sander, Phys. Rev. Lett. **47**, 1400 (1981).
[11] D. Wilkinson and J. Willemsen, J. Phys. A **16**, 3365 (1983).
[12] M. Dias and D. Wilkinson, J. Phys. A **19**, 3131 (1986).
[13] L. Furuberg, J. Feder, A. Aharony, and T. Jossang, Phys. Rev. Lett. **61**, 2117 (1988).
[14] S. Roux and E. Guyon, J. Phys. A **22**, 3693 (1989).
[15] K. Sneppen, Phys. Rev. Lett. **69**, 3539 (1992); K. Sneppen and M.H. Jensen, *ibid.* **71**, 101 (1993).
[16] A.P. Sheppard, M.A. Knackstedt, W.V. Pinczewski, and M. Sahimi, J. Phys. A **32**, L521 (1999).
[17] M.A. Knackstedt, M. Sahimi, and A.P. Sheppard, Phys. Rev. E **61**, 4920 (2000).
[18] S. Schwarzer, A. Shlomo, and A. Bunde, Phys. Rev. E **59**, 3262 (1999).
[19] F. Family and T. Viscek, J. Phys. A **18**, L75 (1985).
[20] S. Havlin, L.A.N. Amaral, S.V. Buldyrev, S.T. Harrington, and H.E. Stanley, Phys. Rev. Lett. **74**, 4205 (1995).
[21] J.M. López, M.A. Rodríquez, and R. Cuerno, Phys. Rev. E **56**, 3993 (1997).
[22] J. Krug, Phys. Rev. Lett. **72**, 2907 (1994).
[23] We note that $\alpha > 1$ for the distribution to be normed, and that $\alpha > 3$ leads asymptotically to the Gaussian distribution [5].